should be turned.

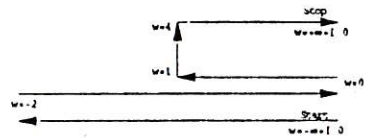

Fig. 6

4. DRAWING THE CORRECT GEOMETRY

Only the last of the angles gave us a problem. The principal values again are $\{\pi, 0, \pi, -\pi/2, 0\}$. However with $w = -3$ we found:

$$\Delta z = \frac{\sqrt{-3-1}\sqrt{-3-4}}{-3(-3+2)}\Delta w = \frac{2\sqrt{7}}{3} \prec -180^0 \Delta w \qquad (17)$$

This is the correct angle, but *not* the principal value. Thus the correct angles are obtained in the following simple way: each singularity gives its own information separately and should not be disturbed from what happens near the other singularities far away. We therefore calculate the correct angles:

```
angle[ w_] = Arg[√(w-1)] + Arg[√(w-4)] - Arg[w+2] - Arg[w] ;
{ angle[-3], angle[-1], angle[0.5], angle[2], angle[5] }
```

$$\left\{-\pi,\ 0,\ \pi,\ \frac{\pi}{2},\ 0\right\} \qquad (18)$$

A simple plot would be:

```
Plot[ angle[w], {w, -4, 6}, PlotLabel = "Schwarz-Christoffel"] ;
```

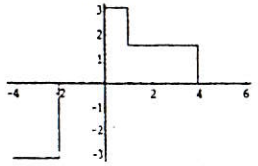

Fig. 7

The geometric implementation walking in the *z-plane* leads to the following route: 1) *west* – 2) turn +180° and walk *east* – 3) turn +180° and walk *west* – 4) then *north* – 5) then *east*. And the correct drawing in the *z-plane* is shown below.

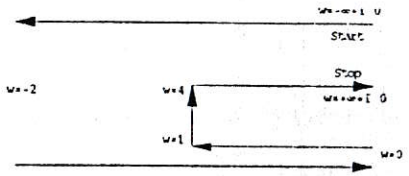

Fig. 8

This corresponds to the geometry in [2]. Which programming tricks the authors have used to obtain the correct magnetic field is not the main message in their paper.

After integration we have $B + A\int \frac{dz}{dw} dw$.

The complex constants A or B do not influence the physical shape of the field. The constant A only magnifies and rotates, B only translates the drawing.

5. CONCLUSION

As we with Schwarz-Christoffel moves to the left in the mathematical *w-plane*, the more composed will the complex arguments of the involved derivative *(dz/dw)* be. Using principal values in computers lead to wrong angles. We saw how to chose the correct angle.

How much more would it be to choose the correct - complicated - antidevative from an ambiguous derivative! As far as known Schwarz-Christoffel did not give us an integral, only a derivative.

This leads to the conclusion that solving the Laplacian should be done with numerical methods.

As a consequence a search on the Internet [3] indicates that this idea already is being realised.

6. REFERENCES

[1] Nielsen M., Munteanu C., " Modified Schwarz - Christoffel Transformation", *Acta Electrotehnica Napocensis*, Vol. 38, No.1, 1997.

[2] Petrean L., Peter D. C., "The Estimation of the Gradient Magnetic Forces by the Conformal Transformation Method", *Proceedings of the CADEMEC '97 Conference*, Cluj-Napoca, Aug. 1997.

[3] http: // amath.colorado.edu/appm/faculty/tad/SC-toolbox/

DETERMINATION OF ELECTROMAGNETIC TORQUE OF AN 8/6 SWITCHED RELUCTANCE MOTOR

Viorel Trifa, Richard Marschalko, Ramona Gălătuş, Ambruş Szekely

Technical University of Cluj-Napoca, Department of Electrical Drives and Robots, Romania
E-mail: trifa@edr.utcluj.ro

ABSTRACT: The paper proposes an analytical determination of electromagnetic torque of an 8/6 switched reluctance motor (SRM) starting from magnetisation curves. In this purpose the method of current decay is chosen and the LabVIEW with HiQ environment is used for data acquisition and processing. Theoretical results are confronted with experimental ones.

1. INTRODUCTION

On the basis of electromagnetic parameter determination are SRM magnetisation curves, using current decay for a given position of the rotor [1]. In this purpose the motor is placed on a rotary table which allows rotor deviating in respect to stator position with a precision of seconds order. One of the motor phases is commutated in report with an adjustable and filtered D.C. source, through an intermediary circuit with a transistor, resistor and suppressing diode, like in figure 1.

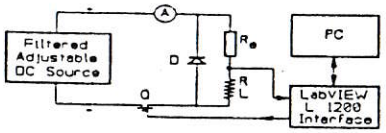

Fig. 1. Set-up arrangement for current decay acquisition.

The transistor control is given through a PC-based labVIEW data acquisition system, L1200 [2], via one of its digital outputs. It is used an analogue input channel of labVIEW board for exponential current acquisition at the phase disconnecting. In this purpose an integrated current transducer, LEM of LA 55-P/SP1 type is used. At the same time the current values are stored in an ASCII file. There are aquisitioned and stored currents between 2-12 A range, with a step of 2A, at different rotor positions between 0° (aligned position) and 30° (unaligned position), with a step of 3°. Totally result 6x11=66 ASCII files and each of them stores current decay waveform. The noise from suppressing circuit influences the data measurement accuracy. Figure 2 shows the current decay curve obtained, at two different scales, with a sampling period of 0.1 ms (10kHz), on 10000 samplings (1 sec).

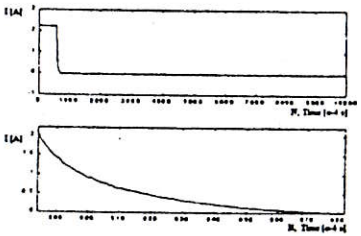

Fig. 2. Acquisitioned decaying current.

2. MAGNETIZATION CURVES

The $\Psi(i,\theta)$ curves family is obtained from the voltage equation in suppressing circuit of the phase:

$$\psi = \int_0^{\infty} (V - Ri)dt \qquad (1)$$

where Ψ is total flux of the phase (flux linkage) and R is the sum of resistances along the suppressing circuit including phase resistance and additional resistance R_e, with the condition $V = 0$. The integral calculus is made in HiQ environment [3] for each current waveform stored in the form that is shown in figure 2. It is obtained the plane, 2D and

spatial representation, 3D of magnetisation curves and they are shown in figures 3a and b respectively.

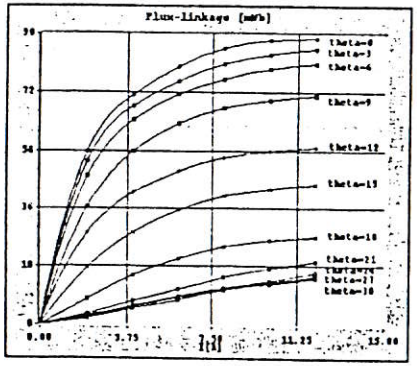

a)

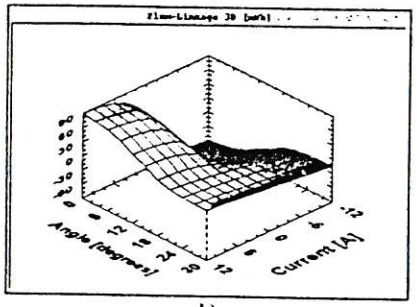

b)

Fig. 3. Magnetization curves (a) and surface (b)

The effect of saturation is also observed, beginning with medium values of current and periodical dependence of flux-linkage with rotation angle. It is taken into account the symmetry of SRM magnetic characteristics related to extreme positions of the rotor in respect with stator position (aligned and unaligned positions).

3. PHASE INDUCTIVITIES

The motor that is tested is a 4-phase 8/6 SRM [4,5]. The 8 stator poles are wound so that each phase consists in two diametrically opposite windings. This 4-phase arrangement determines mutual inductivities practically null. In this situation the measured inductivity is equal with phase inductivity.

In nonlinear electromagnetic systems it is defined two kinds of inductivities: static and dynamic. The static inductivity is given by the expression:

$$L(i,\theta) = \frac{\psi(i,6)}{i} \qquad (2)$$

and dynamic inductivity by the expression:

$$l(i,\theta) = \frac{d\psi(i,6)}{di}\Big|_{\theta=const.} \qquad (3)$$

Both of them are used for SRM modelling and are included in voltage equation of phases. Figures 4 a and b indicate the variation of static and dynamic inductivity versus current and position. The processing of their values are obtained in HiQ environment.

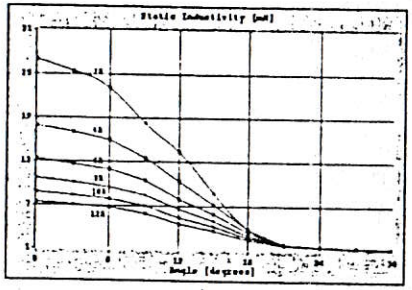

a)

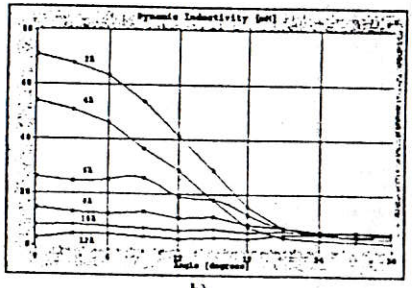

b)

Fig. 4. Static (a) and Dynamic (b) inductivities.

It is observed the increasing dependencies of inductivities in respect to current and position. Magnetic saturation strongly affects the static and dynamic values of inductivities.

4. MAGNETIC COENERGY

To determine each phase contribution to produce electromagnetic torque, it is calculated

the coenergy of one phase supply, with expression:

$$W(i,\theta) = \int_0^i \psi(i,\theta)di \qquad (4)$$

which represents the aria below $\Psi(i)$ curves until a given current, for each rotor position. The coenergy variation, which is calculated in HiQ environment with this expression, is given in figures 5 a and b, taking in account the symmetry of SRM magnetic circuit.

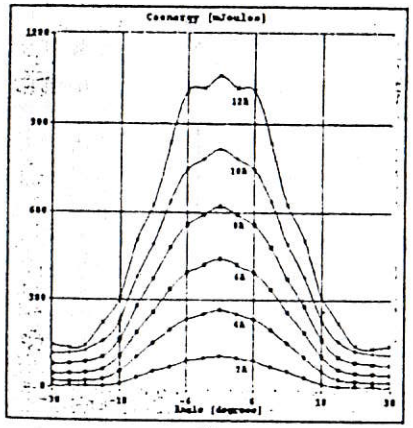

a)

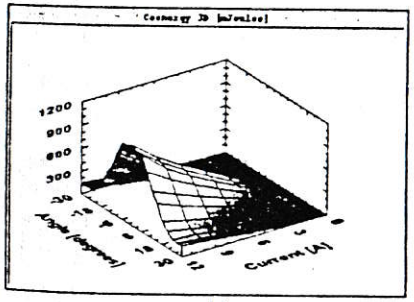

b)

Fig. 5. Coenergy curves (a) and surface (b).

5. ELECTROMAGNETIC TORQUE

The expression of electromagnetic torque results from the Theorem of Generalised Forces:

$$M_e = \frac{dW(i,6)}{d6}\Big|_{i=const} \qquad (5)$$

Electromagnetic torque variation versus phase current and rotation angle results by differentiating the expression of coenergy. 2D and 3D representations of torque are shown in figures 6 a and b.

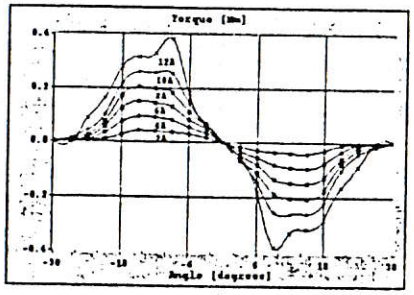

a)

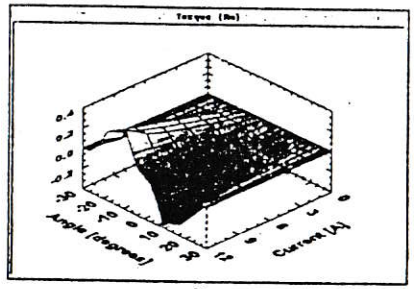

b)

Fig. 6. Electromagnetic torque curves (a) and surface (b).

It is observed unsinusoidal variation of electromagnetic torque versus position, but periodical and symmetrical behaviour versus unaligned rotor position.

The electromagnetic torque determining began with a trial as described in this paper. The calculated values can be comparated through an experimental trial of static torque developed by this motor. In figure 7 it is given electromagnetic torque curves for a phase current of 10A.

It is found a good overlap of calculated results in HiQ environment with that which is directly obtained by torque measurement and this fact certifies rigorous calculus and experimental trial that was made.

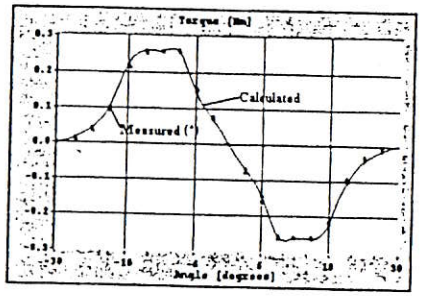

Fig. 7. Measured and calculated torque.

6. CONCLUSIONS

Using virtual instrumentation from labVIEW environment, joined with HiQ permits not just an experimental investigation at professional level, but a friendly and high level graphical processing of acquisitioned data.

In the particular case of SRM, virtual instrumentation resolves a difficult and inefficient problem until now from data processing point of view, that of determining the magnetic characteristics with an acceptable precision. This characteristics make up an auspicious premise for a rigorous and comprehensive modelling of SRM electrical drive behaviour. On the other hand the characteristics that are obtained release a solid support for validating the analysed results through FED, which is applied in general, at the present time, in electrical machines design.

7. REFERENCES

[1] Miller, T.J.E. *Switched Reluctance Motors and Their Control*. Magna Physics Pub., Clarendon Press, Oxford, 1993.

[2] *** LabVIEW User's Guide. National Instruments, 1998.

[3] *** HiQ Reference Manual. National Instruments, 1998

[4] Trifa, V., Marschalko, R., Szasz, Cs., Szekely, A., Gălătuş Ramona "Investigation of a four-phase switched reluctance motor supplied from a PWM inverter". *Proceedings of OPTIM'98 Conference*, Braşov, Romania, 1998, pp. 341-344.

[5] Trifa, V., Gălătuş Ramona, Szekely, A., Szasz, Cs. "Aspects concerning the commutation of 8/6 switched reluctance motors". *Proceeding of Electromotion Conference*, Patras, Greece, July 1999, pp. 125-130.

THE NUMERICAL SIMULATION OF THE STEADY-STATE SKIN EFFECT USING THE BOUNDARY ELEMENTS METHOD

Calin Munteanu [1], Emil Simion [1], Vasile Topa [1], Laura Fogarasi [1]
Gilbert De Mey [2], Johan Deconinck [3]

[1] *Technical University of Cluj-Napoca, Electrotechnics Department, Romania, E-mail: calinm@et.utcluj.ro*
[2] *University of Gent, Electronics and Information Systems Department, Belgium*
[3] *Free University of Brussels VUB, Department of Electrical Engineering, Belgium*

ABSTRACT: The paper presents the Boundary Elements Method (BEM) utilisation in the numerical analysis of the steady-state electromagnetic field diffusion effects. In the beginning, the basic quasi-static electromagnetic field equations in the terms of the magnetic vector potential will be presented. The numerical implementation of the BEM will be detailed afterwards. Several examples of skin effect analysis will be presented. Few conclusions will end the paper.

1. INTRODUCTION

This paper presents the numerical analysis of the electromagnetic field diffusion effects in steady-state sinusoidal regime. Assuming that the current carrying conductor is straight and very long, the problem is treated in the conductor's cross-section as a 2D equivalent domain. The main objective of this analysis is to determine the total current distribution inside the conductor when the eddy currents are taken into consideration and the way this distribution affects the losses and performances of the conducting system.

In order to determine the current distribution in the conductors' cross-section due to the diffusion effects the interior and exterior problems must be solved simultaneously. This task is difficult to be handled by the 'domain numerical methods' like Finite Elements or Finite Differences due to the infinite extension of the conductors' outer dielectric space. Usually these methods assumed a large enough bounded domain with zero Dirichlet boundary conditions, but this assumption leads to solution accuracy lose and also to a high amount of computational work.

The Boundary Elements Method is more suitable to be used for this kind of problems because it requires the discretization of the conductor's boundary only, simultaneously solving the interior and exterior governing equations. Moreover, the outer space is not considered arbitrary bounded, the method allowing to find the electromagnetic quantities from the infinitely extended domain.

2. BASIC EQUATIONS

The start equation in the study of the electromagnetic diffusion in conductive media in terms of the vector potential formulation is given by [1], [2]:

$$\nabla\times\left(\frac{1}{\mu}\nabla\times\overline{A}\right)=-\sigma\left(\frac{\partial\overline{A}}{\partial t}+\nabla\Phi\right) \qquad (1)$$

Using the 2D equivalent working domain the Coulomb gauge is automatically satisfied [1] taking into consideration that in this case $\overline{A}=A(x,y)\overline{k}$ and thus equation (1) becomes:

$$-\frac{1}{\mu}\Delta\underline{A}=-j\omega\sigma\underline{A}-\sigma\nabla\underline{\Phi} \qquad (2)$$

Due to the fact that the electric scalar potential $\Phi(z)$ along a straight conductor of arbitrary cross section represents a gradient field as shown in Figure 1, it must satisfy the Laplace equation and its solution can be expressed as [1]:

$$\Phi(z)=\frac{\Phi(l)-\Phi(0)}{l}z+\Phi(0) \qquad (3)$$